

An introduction to extended dynamic mode decomposition: Estimation of the Koopman operator and outputs

Nibodh Boddupalli

December 2020

Many physical systems exhibit phenomena with unknown governing dynamics. These systems can be high dimensional and often partially observed. Recently, an emerging set of operator-theoretic tools have gained traction, centered on discovering linear representations or approximations of nonlinear dynamical systems in function spaces [1, 2]. Originally derived for Hamiltonian systems [3], popular numerical [4, 5, 6, 7] and theoretical [8] techniques for Koopman operator theory enable input-output perspective [9, 10, 11], and spectral analysis of nonlinear systems [2, 12].

One of the primary interests in the development [1, 2] and further exploration [8, 13] of Koopman operator framework is its relations to the properties of the underlying dynamical systems as demonstrated in [14, 9, 12], etc. For this, we briefly introduce the Koopman operator without delving into its spectral properties in section 1. We then present vector and matrix representations of observables and the Koopman operator as a projection onto some finite-dimensional function space without assumptions of its invariance to the action of the Koopman operator or spanning the outputs in section 2 which is the basis for the extended dynamic mode decomposition (EDMD) algorithm [6]. EDMD is a modal decomposition algorithm which is a popular numerical method for obtaining finite-sections of the Koopman operator that has proved useful for predictions and control in nonlinear systems [10, 15]. We also include output data containing both expected and unknown observables. This work is largely adapted from [16].

1 Koopman perspective of dynamical systems

The initial use of composition operator on square-integrable functions of state evolving under measure-preserving flows [3]. The mathematical framework developed in much recent years like [1, 2, 8] has broadened applicability with relaxed regularity conditions to include hybrid systems [17], switched systems [18], stochastic systems [13], etc. This shows that the framework is applicable even when the flow is not smooth and the state-dynamics are discontinuous.

The theory of infinite-dimensional linear operators has been developed alongside studies on distributed systems [19]. The Koopman operator is a linear operator with proven relationship to the spectral properties of the underlying nonlinear systems in [1, 2] and more recently in [8]. However, we will be focusing on the computational implementation after a brief introduction to the theory. For detailed definitions and regularity conditions, we direct the readers to [20].

Consider a state $\mathbf{x} \in \mathcal{M} \subseteq \mathbb{R}^n$ whose evolution in time $t \in \mathbb{R}_{\geq 0}$ is given by the non-singular flow of a dynamical system $\mathbf{S}^t : \mathcal{M} \rightarrow \mathcal{M}$ as

$$\mathbf{x}(t) = \mathbf{S}^t(\mathbf{x}(0)). \tag{1.1}$$

The functions of state $g : \mathcal{M} \rightarrow \mathbb{C}$ in Koopman operator literature are called “observables”. While observations are real-valued, complex-valued functions allow inclusion of eigenfunctions of the Koopman operator as seen later. If an observable g belongs to a function space \mathcal{F} which is closed under composition \circ with \mathbf{S}^t , the Koopman operator (family) $\mathcal{K}^t : \mathcal{F} \rightarrow \mathcal{F}$ associated with system 1.1 is defined as

$$\mathcal{K}^t g = g \circ \mathbf{S}^t. \tag{1.2}$$

While we used $\mathbf{x}(0)$ for illustration, note that the state can be dropped from the equations with the Koopman operator (like equation (1.2)) giving a *global* perspective on the state-space using observables. Examples of observables include functions of state like a state-variable $g_1(\mathbf{x}) = x_2$, an output $g_2(\mathbf{x}) =: y$, possible basis functions like $g_3(\mathbf{x}) = |x_1 - c_i|^2 \log |x_1 - c_i| =: \psi_i(\mathbf{x})$, etc. [20]. The Koopman operator (family) \mathcal{K}^t exists and is unique if the map \mathbf{S}^t exists and is unique. For this and other properties [20] offers further references.

The linearity of the Koopman operator (semigroup) comes from the linearity of composition as seen from

$$\mathcal{K}^t(\alpha_1 g_1 + \alpha_2 g_2) = (\alpha_1 g_1 + \alpha_2 g_2) \circ \mathcal{K}^t = \alpha_1 g_1 \circ \mathcal{K}^t + \alpha_2 g_2 \circ \mathcal{K}^t = \alpha_1 (\mathcal{K}^t g_1) + \alpha_2 (\mathcal{K}^t g_2), \quad (1.3)$$

with $\alpha_1, \alpha_2 \in \mathbb{R}$. The trade-off for linearity is dimensionality as the Koopman operator (semigroup) is usually infinite-dimensional since its domain is an $L^p(\mathcal{M})$ space but in data-driven algorithms, we restrict its action to finite-dimensional spaces as seen later. In particular, we will work in a Hilbert space so $\mathcal{F} = L^2(\mathcal{M})$ and $\mathcal{K}^t : L^2(\mathcal{M}) \rightarrow L^2(\mathcal{M})$. Since we deal with data-points sampled discretely in time at intervals of Δt , we use the map $\mathbf{S} := \mathbf{S}^1$ or $\mathbf{S}^{\Delta t}$

$$\mathbf{x}^+ = \mathbf{S}(\mathbf{x}) \quad (1.4)$$

and the corresponding discrete Koopman operator formulation $\mathcal{K} := \mathcal{K}^1$ or $\mathcal{K}^{\Delta t}$

$$\mathcal{K}g = g \circ \mathbf{S}. \quad (1.5)$$

2 Finite-dimensional representations of the Koopman operator and observables

A popular approach to representing the Koopman operator is extended dynamic mode decomposition (EDMD) [6] which is a Galerkin method [15] also known as a finite-section method [21]. Along these lines, we use a finite number of observables $\{\psi_i\}_{i=1}^{n_L} : \mathcal{M} \rightarrow \mathbb{R}$ in a Hilbert space $\mathcal{F} = L^2(\mathcal{M})$. The space spanned by these observables $\tilde{\mathcal{F}} := \text{span}\{\psi_1, \psi_2, \dots, \psi_{n_L}\}$ is a n_L -dimensional subspace of the Hilbert space $\tilde{\mathcal{F}} \subset \mathcal{F}$. These n_L observables are a basis for $\tilde{\mathcal{F}}$ and are often called “dictionary functions” in literature.

2.1 Vector representation of an observable

For any $g \in \tilde{\mathcal{F}}$,

$$g(\mathbf{x}) = \sum_{i=1}^{n_L} w_i \psi_i(\mathbf{x}) \quad (2.6)$$

for some coefficients $\{w_i\}_{i=1}^{n_L}$. By denoting the coefficients and basis as vectors, we can drop the summation symbols. Denoting

$$\boldsymbol{\psi}(\mathbf{x}) := \begin{bmatrix} \psi_1(\mathbf{x}) \\ \vdots \\ \psi_{n_L}(\mathbf{x}) \end{bmatrix} \quad \mathbf{w} := \begin{bmatrix} w_1 \\ \vdots \\ w_{n_L} \end{bmatrix},$$

equation (2.6) can be rewritten as

$$g(\mathbf{x}) = \boldsymbol{\psi}(\mathbf{x})^T \mathbf{w} \quad (2.7)$$

where $(\cdot)^T$ denotes the transpose. This representation of the observable remains unchanged with the argument, allowing us to drop \mathbf{x} and make the equations concise.

2.2 Matrix representation of the Koopman operator

If the action of the infinite-dimensional Koopman operator on a Hilbert space $\mathcal{K} : L^2(\mathcal{M}) \rightarrow L^2(\mathcal{M})$ is invariant to a subspace in its domain $\tilde{\mathcal{F}} \subset L^2(\mathcal{M})$ i.e. $g \in \tilde{\mathcal{F}} \Rightarrow \mathcal{K}g \in \tilde{\mathcal{F}}$, then its restriction to that subspace $\mathcal{K}_{\tilde{\mathcal{F}}}$ has a finite-dimensional representation as a matrix [22]. Similar to that taken in [6], this ensures that the composition of an observable g with the map \mathbf{S} lies in the span of the basis. Then, using equation (2.7) in equation (1.5), let

$$\mathcal{K}g = g \circ \mathbf{S} = \boldsymbol{\psi}^T \mathbf{w}^+, \quad (2.8)$$

for some $\mathbf{w}^+ := [w_1^+, w_2^+, \dots, w_{n_L}^+]^T$ (following notation of equation (1.4)) as the vector of coefficients in the basis expansion of $g \circ \mathbf{S}$. The left hand side can be rewritten as an expansion like that in equation (2.6):

$$\mathcal{K}g = \mathcal{K} \sum_{i=1}^{n_L} w_i \psi_i = \sum_{i=1}^{n_L} w_i \mathcal{K}\psi_i = \begin{bmatrix} \mathcal{K}\psi_1 & \dots & \mathcal{K}\psi_{n_L} \end{bmatrix} \mathbf{w}. \quad (2.9)$$

From invariance, each $\{\mathcal{K}\psi_i\}_{i=1}^{n_L}$ is a linear combination of the basis and can also be represented as

$$\mathcal{K}\psi_i =: \boldsymbol{\psi}^T \mathbf{k}_i. \quad (2.10)$$

Using equation (2.10) in (2.9),

$$\mathcal{K}g = \boldsymbol{\psi}^T \begin{bmatrix} | & & | \\ \mathbf{k}_1 & \dots & \mathbf{k}_{n_L} \\ | & & | \end{bmatrix} \mathbf{w} =: \boldsymbol{\psi}^T (\mathbf{K} \mathbf{w}). \quad (2.11)$$

Here, $\mathbf{K} \in \mathbb{R}^{n_L \times n_L}$ can be viewed as the restriction of the Koopman operator to the subspace $\mathcal{K}_{\tilde{\mathcal{F}}}$ called the ‘‘Koopman matrix’’ for convenience. It acts on the observable g represented as \mathbf{w} in basis $\boldsymbol{\psi}$ to give the the composition of the observable with the flow which is the vector \mathbf{w}^+ . From right hand side of equations (2.8, 2.11),

$$\mathcal{K}g = \boldsymbol{\psi}^T(\mathbf{K}\mathbf{w}) = \boldsymbol{\psi}^T\mathbf{w}^+ = g \circ \mathbf{S}. \quad (2.12)$$

2.3 Approximating the Koopman operator

Without assuming invariance i.e. $g \in \tilde{\mathcal{F}} \not\Rightarrow \mathcal{K}g \in \tilde{\mathcal{F}}$, $\mathcal{K}g$ may not be represented as a linear combination of the basis functions so we do not necessarily have a matrix representation of $\mathcal{K} : L^2(\mathcal{M}) \rightarrow L^2(\mathcal{M})$. Since $\tilde{\mathcal{F}}$ is a closed linear subspace of $L^2(\mathcal{M})$, we know from the projection theorem [23] the existence of a unique minimizer $f \in \tilde{\mathcal{F}}$

$$\mathcal{P}(g \circ \mathbf{S}) = \arg \min_{f \in \tilde{\mathcal{F}}} \|f - g \circ \mathbf{S}\|_{L^2(\mathcal{M})}, \quad (2.13)$$

which is the orthogonal projection of $\mathcal{K}g$ onto $\tilde{\mathcal{F}}$ using the projection $\mathcal{P} : L^2(\mathcal{M}) \rightarrow \tilde{\mathcal{F}}$. Here $\|\cdot\|_{L^2(\mathcal{M})}$ is the L^2 norm over \mathcal{M} assuming the usual Borel measure.

From equations (2.9), this projection would be the linear combination of the projections of each of the terms on its right hand side onto the space $\tilde{\mathcal{F}}$:

$$\mathcal{P}(g \circ \mathbf{S}) = \mathcal{P}(\mathcal{K}g) = \mathcal{P}\left(\sum_{i=1}^{n_L} w_i \mathcal{K}\psi_i\right) = \mathcal{P}\left(\begin{bmatrix} \mathcal{K}\psi_1 & \dots & \mathcal{K}\psi_{n_L} \end{bmatrix} \mathbf{w}\right). \quad (2.14)$$

By deriving the normal equations [23] as shown in [16], the above can be written as

$$\mathcal{P}(g \circ \mathbf{S}) = \begin{bmatrix} \mathcal{P}(\mathcal{K}\psi_1) & \cdots & \mathcal{P}(\mathcal{K}\psi_{n_L}) \end{bmatrix} \mathbf{w} = \boldsymbol{\psi}^T \begin{bmatrix} | & & | \\ \tilde{\mathbf{k}}_1 & \cdots & \tilde{\mathbf{k}}_{n_L} \\ | & & | \end{bmatrix} \mathbf{w} =: \boldsymbol{\psi}^T (\tilde{\mathbf{K}} \mathbf{w}), \quad (2.15)$$

where $\tilde{\mathbf{K}} := \mathcal{P}\mathcal{K}$ is obtained as

$$\tilde{\mathbf{K}} = \begin{bmatrix} \langle \psi_1, \psi_1 \rangle & \cdots & \langle \psi_1, \psi_{n_L} \rangle \\ \vdots & \ddots & \vdots \\ \langle \psi_{n_L}, \psi_1 \rangle & \cdots & \langle \psi_{n_L}, \psi_{n_L} \rangle \end{bmatrix}^{-1} \begin{bmatrix} \langle \psi_1, \psi_1 \circ \mathbf{S} \rangle & \cdots & \langle \psi_1, \psi_{n_L} \circ \mathbf{S} \rangle \\ \vdots & \ddots & \vdots \\ \langle \psi_{n_L}, \psi_1 \circ \mathbf{S} \rangle & \cdots & \langle \psi_{n_L}, \psi_{n_L} \circ \mathbf{S} \rangle \end{bmatrix} =: \mathbf{G}^{-1} \mathbf{A}. \quad (2.16)$$

where $\langle \cdot, \cdot \rangle$ is an inner-product assuming the usual Borel measure over \mathcal{M} . As evident from the matrix entries, accuracy of numerical implementations also depends on the approximation of inner-products. The above was already shown as a Galerkin projection in [6] and as Analytic EDMD in [15] along with proofs of convergence.

2.4 Matrix representation of vector observables

The notion of “vector-observables” is presented in Koopman operator literature as a natural extension for multiple observables by stacking them as into a vector [24] like the full-state observables as an identity function $id(\mathbf{x}) = \mathbf{x}$, partial state-observations [5], or multiple outputs from a controlled system $\mathbf{y} = \mathbf{g}(\mathbf{x})$ [10]. Given observables $g_1, g_2, \dots, g_p \in L^2(\mathcal{M})$

$$\left. \begin{array}{l} \mathcal{K}g_1 = g_1 \circ \mathbf{S} \\ \vdots \\ \mathcal{K}g_p = g_p \circ \mathbf{S} \end{array} \right\} \implies \mathcal{K} \begin{bmatrix} g_1 \\ \vdots \\ g_p \end{bmatrix} = \begin{bmatrix} g_1 \\ \vdots \\ g_p \end{bmatrix} \circ \mathbf{S}.$$

If these observables are known like partial-state $\mathbf{g}(\mathbf{x}) = \mathbf{C}\mathbf{x}$, a basis $\text{span}\{\psi_i\}_{i=1}^{n_L} =: \tilde{\mathcal{F}}$ can be chosen such that $g_1, g_2, \dots, g_p \in \tilde{\mathcal{F}}$. Then, each observable has an expansion like that in equation (2.6) and their coefficients of expansion can be written as vectors like in equation (2.7)

$$\mathbf{g}^T := \begin{bmatrix} g_1 & \cdots & g_p \end{bmatrix} = \begin{bmatrix} \boldsymbol{\psi}^T \mathbf{w}_1 & \cdots & \boldsymbol{\psi}^T \mathbf{w}_p \end{bmatrix} = \boldsymbol{\psi}^T \begin{bmatrix} | & & | \\ \mathbf{w}_1 & \cdots & \mathbf{w}_p \\ | & & | \end{bmatrix} =: \boldsymbol{\psi}^T \mathbf{W}, \quad (2.17)$$

where $\mathbf{W} \in \mathbb{R}^{n_L \times p}$ is a matrix representation of the observables. However, the choice of basis is not straightforward even with known observables as it also determines the accuracy of $\tilde{\mathbf{K}}$ as seen in equation (2.16).

2.5 Approximating unknown observables

When the observables are unknown, we project them onto the span of chosen basis $\tilde{\mathcal{F}}$ and approximate them as done when $\mathcal{K}\psi_i \notin \tilde{\mathcal{F}}$ similar to equations (2.15, 2.16):

$$\mathcal{P}(\mathbf{g})^T = \boldsymbol{\psi}^T \begin{bmatrix} | & & | \\ \tilde{\mathbf{w}}_1 & \cdots & \tilde{\mathbf{w}}_p \\ | & & | \end{bmatrix} =: \boldsymbol{\psi}^T \tilde{\mathbf{W}}, \quad (2.18)$$

where $\tilde{\mathbf{W}}$ obtained as

$$\begin{bmatrix} | & & | \\ \tilde{\mathbf{w}}_1 & \cdots & \tilde{\mathbf{w}}_p \\ | & & | \end{bmatrix} = \mathbf{G}^{-1} \begin{bmatrix} \langle \psi_1, g_1 \rangle & \cdots & \langle \psi_1, g_p \rangle \\ \vdots & \ddots & \vdots \\ \langle \psi_{n_L}, g_1 \rangle & \cdots & \langle \psi_{n_L}, g_p \rangle \end{bmatrix} =: \mathbf{G}^{-1} \mathbf{B}, \quad (2.19)$$

uniquely minimizes $\|\boldsymbol{\psi}^T \tilde{\mathbf{w}}_i - g_i\|_{L^2(\mathcal{M})} \forall i = 1, 2, \dots, p$ analogous to equation (2.13).

3 Numerical estimation: EDMD

We introduce the extended dynamic mode decomposition (EDMD) algorithm proposed in [6] to numerically implement the finite-section approximations seen in section 2. Dynamic Mode Decomposition (DMD) was introduced in [25] as a method to approximate modal decomposition of fluid flows. While modal analysis techniques like the Proper Orthogonal Decomposition (POD) existed earlier, DMD does not enforce orthogonality of the modes. The connection of these modes to spectral properties of the Koopman operator was shown in [5] and later in [22].

The accuracy of EDMD not only depends on the user's choice of basis as mentioned in [6] where knowing the desired observables' composition under the Koopman operator would allow us to use them as the dictionary but it also depends on the available data and how it is sampled [15, 16]. In approximating unknown observables and the Koopman operator in Hilbert spaces, we require knowledge of inner products of functions over regions of state-space. In EDMD [6], summations over data-points are used to approximate the inner products which could converge in the limit of large data [15]. Subsequently, kernel methods were used to directly obtain inner products [26]. Such Hilbert spaces endowed with kernels called Reproducing Kernel Hilbert Spaces (RKHS) were further developed for continuous time implementations [27] and control [28] but is beyond the scope of EDMD as introduced in [6] which was the topic of results in [16].

3.1 Numerical estimation of the Koopman operator

Numerical estimation of the Koopman matrix is not far from the analytical expressions in section 2 in sense that we want residuals to be minimized in $\|\cdot\|_{L^2}$. From equation (2.16)

$$\tilde{\mathbf{K}} = \mathbf{G}^{-1} \mathbf{A},$$

accuracy of the numerical estimations $\tilde{\mathbf{K}}$ would depend on our approximations of the inner products that are entries of \mathbf{G} and \mathbf{A} . Ideally, these would be calculated over the entire set of states that the dynamical system takes which is \mathcal{M} . If we want to consider only a subset $\mathcal{M}_k \subset \mathcal{M}$, we can use a measure μ_k supported *only* on \mathcal{M}_k as

$$\langle g_i, g_j \rangle = \int_{\mathcal{M}} g_i^*(\mathbf{x}) g_j(\mathbf{x}) \mu_k(\mathbf{x}) d\mathbf{x} = \int_{\mathcal{M}_k} g_i^*(\mathbf{x}) g_j(\mathbf{x}) \mu(\mathbf{x}) d\mathbf{x},$$

where $(\cdot)^*$ denotes complex-conjugate that is needed if observables are eigenfunctions which can be complex [9]. However finite amounts of discretely sampled data changes the sets over which the inner-products are estimated [15]. Consider the following set of states in \mathcal{M}

$$\mathbf{X} := \{\mathbf{x}_1, \mathbf{x}_2, \dots, \mathbf{x}_m\}.$$

An empirical measure $\mu_{\mathbf{X}}$ can be defined over these points using Dirac measure $\delta_{\mathbf{x}_i}$ centered at each \mathbf{x}_i as done in [15]

$$\mu_{\mathbf{X}} = \frac{1}{m} \sum_{i=1}^m \delta_{\mathbf{x}_i},$$

with

$$\langle g_i, g_j \rangle_{\mu_{\mathbf{X}}} = \int_{\mathcal{M}} g_i^*(\mathbf{x}) g_j(\mathbf{x}) \mu_{\mathbf{X}}(\mathbf{x}) d\mathbf{x} = \frac{1}{m} \sum_{k=1}^m g_i^*(\mathbf{x}_k) g_j(\mathbf{x}_k). \quad (3.20)$$

We denote other another set \mathbf{X}^+ (following notation of equation (1.4)) as and values of the basis functions at those points in \mathbf{X} , \mathbf{X}^+ as matrices $\Psi(\mathbf{X}), \Psi(\mathbf{X}^+) \in \mathbb{R}^{m \times n_L}$

$$\begin{aligned} \mathbf{X}^+ &:= \mathbf{S}(\mathbf{X}) = \{\mathbf{S}(\mathbf{x}_1), \mathbf{S}(\mathbf{x}_2), \dots, \mathbf{S}(\mathbf{x}_m)\} \\ \Psi(\mathbf{X}) &:= \begin{bmatrix} \boldsymbol{\psi}(\mathbf{x}_1)^T \\ \vdots \\ \boldsymbol{\psi}(\mathbf{x}_m)^T \end{bmatrix} \quad \Psi(\mathbf{X}^+) := \begin{bmatrix} \boldsymbol{\psi}(\mathbf{S}(\mathbf{x}_1))^T \\ \vdots \\ \boldsymbol{\psi}(\mathbf{S}(\mathbf{x}_m))^T \end{bmatrix} \end{aligned}$$

Using equation (3.20), the estimate for the matrix entries of \mathbf{G} , \mathbf{A} are:

$$\begin{aligned} G_{ij} &= \langle \psi_i, \psi_j \rangle_{\mu_{\mathbf{X}}} = \frac{1}{m} \sum_{k=1}^m \psi_i^*(\mathbf{x}_k) \psi_j(\mathbf{x}_k) \implies \mathbf{G} = \frac{1}{m} \Psi(\mathbf{X})^* \Psi(\mathbf{X}) \\ A_{ij} &= \langle \psi_i, \psi_j \circ \mathbf{S} \rangle_{\mu_{\mathbf{X}}} = \frac{1}{m} \sum_{k=1}^m \psi_i^*(\mathbf{x}_k) \psi_j(\mathbf{S}(\mathbf{x}_k)) \implies \mathbf{A} = \frac{1}{m} \Psi(\mathbf{X})^* \Psi(\mathbf{X}^+) \end{aligned} \quad (3.21)$$

where $\Psi(\mathbf{X})^*$ denotes complex-conjugate transpose of $\Psi(\mathbf{X})$. Using the above, the numerically estimated $\tilde{\mathbf{K}}$ using equation (2.16) is

$$\tilde{\mathbf{K}} = \mathbf{G}^{-1} \mathbf{A} = \left(\frac{1}{m} \Psi(\mathbf{X})^* \Psi(\mathbf{X}) \right)^{-1} \frac{1}{m} \Psi(\mathbf{X})^* \Psi(\mathbf{X}^+) = \Psi(\mathbf{X})^\dagger \Psi(\mathbf{X}^+),$$

where $(\cdot)^\dagger$ is the Moore-Penrose (MP) Pseudoinverse. This is the form commonly presented as the interpretation of the Koopman matrix being the best approximation of the flow as a linear map since this minimizes the residual

$$\begin{aligned} \min \|\mathcal{K}\psi_i - \boldsymbol{\psi}^T \tilde{\mathbf{k}}_i\|_{L^2(\mu_{\mathbf{X}})} \text{ for each } i = 1, 2, \dots, n_L \\ \implies \min \|\Psi(\mathbf{X}^+) - \Psi(\mathbf{X}) \tilde{\mathbf{K}}\|_F. \end{aligned} \quad (3.22)$$

This gives an exact representation (i.e. 0 residual in $\|\cdot\|_{L^2(\mu_{\mathbf{X}})} \forall i = 1, \dots, n_L$) of the Koopman operator if our chosen basis $\{\psi_i\}_{i=1}^{n_L}$ spans $\{\mathcal{K}\psi_i\}_{i=1}^{n_L}$ over \mathbf{X} .

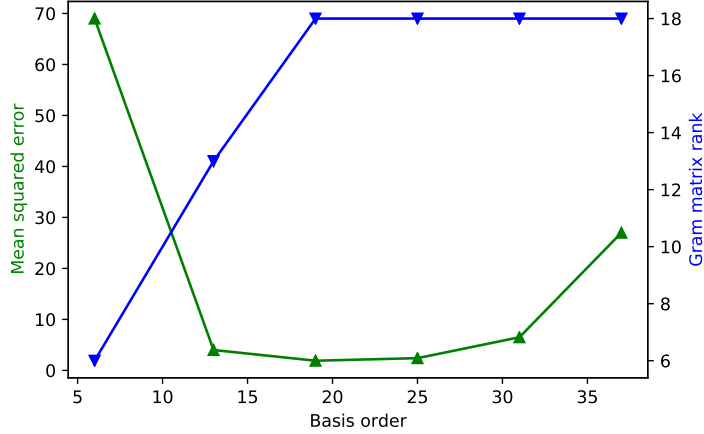


Figure 3.1: Example of effect of dictionary and \mathbf{X} on rank of \mathbf{G} and residual. Here, Hermite polynomials on the repressilator [16]

Key assumption in the above is that the Gram matrix \mathbf{G} is invertible [15]. This happens only if the dictionary is linearly independent over \mathbf{X} , thus forming a basis for $\tilde{\mathcal{F}}$. In case of insufficient data i.e. $m < n_L$ or redundant data like from a period- k fixed-point with $k < n_L$, the Gram matrix is degenerate even if the dictionary functions are linearly independent over \mathbf{X} . So the condition is $\text{rank}(\Psi(\mathbf{X})) = n_L$ [16]. EDMD does not assume that the chosen dictionary of observables is a basis for function space $\tilde{\mathcal{F}}$ that they span over the set \mathbf{X} . For a dictionary that is not necessarily linearly independent, we use the MP-pseudoinverse as shown in [6]

$$\tilde{\mathbf{K}} = \mathbf{G}^\dagger \mathbf{A}. \quad (3.23)$$

which still solves equation (3.22) when the system of equations are over-determined. When the dictionary functions are linearly independent, \mathbf{G} is invertible and $\mathbf{G}^\dagger = \mathbf{G}^{-1}$. When under-determined like in the case of linearly dependent dictionary functions or insufficient data, a continuous family of minimizers exists and the MP-pseudoinverse provides the one with the minimum norm via (truncated) Singular Value Decomposition

(SVD) [23]. When equation (3.22) is solved under constraints on entries of $\tilde{\mathbf{K}}$, it results in regularization. For example, L^2 -regularization [29] can be used to analytically solve

$$\begin{aligned} \min \|\mathcal{K}\boldsymbol{\psi}_i - \boldsymbol{\psi}^T \tilde{\mathbf{k}}_i\|_{L^2(\mu_{\mathbf{X}})} + \lambda \|\tilde{\mathbf{k}}_i\|_2 \text{ for each } i = 1, 2, \dots, n_L \\ \implies \min \|\Psi(\mathbf{X}^+) - \Psi(\mathbf{X})\tilde{\mathbf{K}}\|_F + \lambda \|\tilde{\mathbf{K}}\|_F, \end{aligned} \quad (3.24)$$

using

$$\tilde{\mathbf{K}} = (\mathbf{G} + \lambda \mathbf{I})^{-1} \mathbf{A},$$

where $\lambda \geq 0$ is a "regularizer" that relates to the desired optimization constraint [30].

3.2 Numerical estimation of unknown outputs

In Koopman operator literature, observables are functions of state within the domain of the Koopman operator. Outputs are also observables by definition [20, 10, 9]. We denote the output data as

$$\mathbf{Y} := \begin{bmatrix} \mathbf{y}_1 & \mathbf{y}_2 & \dots & \mathbf{y}_m \end{bmatrix} \in \mathbb{R}^{p \times m}$$

where $\mathbf{y}_i = \mathbf{g}(\mathbf{x}_i)$ since the closed form of output $\mathbf{g}(\mathbf{x})$ is not known. We repeat the procedure for estimating $\tilde{\mathbf{K}}$. we refer to equation (2.19) and use the above to estimate \mathbf{B} like that in equation (3.21) –

$$\mathbf{B} = \frac{1}{m} \Psi(\mathbf{X})^* \mathbf{Y}^T,$$

and get

$$\tilde{\mathbf{W}} = \mathbf{G}^\dagger \mathbf{B} \quad (3.25)$$

which solves

$$\begin{aligned} & \min \|g_i - \boldsymbol{\psi}^T \tilde{\mathbf{w}}_i\|_{L^2(\mu_{\mathbf{X}})} \text{ for each } i = 1, 2, \dots, p \\ & \implies \min \|\mathbf{Y}^T - \boldsymbol{\Psi}(\mathbf{X})\tilde{\mathbf{W}}\|_F. \end{aligned}$$

3.3 Regularization and expected outputs

Regularization can be used here also to minimize the above residual subject to constraints from apriori experience. As outputs are often determined by sensors from high dimensional systems like velocities at some spatial position [4, 5, 7] or even from control systems [10, 9], we can guess some possible forms like $\mathbf{y} = \mathbf{C}\mathbf{x}$ which can be included in the dictionary alongside other possible basis [31, 32]. Consider a dictionary

$$\boldsymbol{\psi}^T = \left[(\mathbf{C}\mathbf{x})^T \quad \mathbf{z}_d(\sigma(\mathbf{z}_{d-1}(\sigma(\dots(\sigma(\mathbf{z}_1))\dots)))^T \right]$$

where $\mathbf{z}_d = \mathbf{H}_d\mathbf{x} + \mathbf{r}_d \in \mathbb{R}^{n_L-p}$ with d being the depth of a neural network with activation functions σ that are known to demonstrate universal function approximation property (UFAP) in practice like rectified linear units [33], sigmoidal functions [34], radial basis functions (RBFs) [35], etc. However, universal function approximators in the dictionary could approximately/exactly span our desired functions that are also in the dictionary [16] causing ill-conditioned/degenerate \mathbf{G} .

In this case, we can use Tikhonov regularization [36] which is broader than the ridge regression used in equation (3.24) to take expected vector representations of outputs into account. Using the above example, we desire $\tilde{\mathbf{W}}$ which solves

$$\min \|\mathbf{c}_i^T \mathbf{x} - \boldsymbol{\psi}^T \tilde{\mathbf{w}}_i\|_{L^2(\mu_{\mathbf{X}})} \text{ for } 1 \leq i \leq p.$$

We expect $\tilde{w}_i^T \approx \left[\mathbf{c}_i^T \quad \mathbf{0}^T \right]$ but the minimum norm solution using equation (3.25) could be different. Consider expected vector representations of first l outputs as $\mathbf{w}_1^0, \mathbf{w}_2^0, \dots, \mathbf{w}_l^0, 1 \leq$

$l \leq p$ and further constraining the sum of their squares using $\|\tilde{\mathbf{w}}_i\|_{\mathbf{Q}} = \tilde{\mathbf{w}}_i^T \mathbf{Q} \tilde{\mathbf{w}}_i$ while we lack apriori information on the rest $p - l$ outputs

$$\begin{aligned} \min \|g_i - \boldsymbol{\psi}^T \tilde{\mathbf{w}}_i\|_{L^2(\mu_{\mathbf{X}})} + \begin{cases} \|\tilde{\mathbf{w}}_i - \mathbf{w}_i^0\|_{\mathbf{Q}} \text{ for } i = 1, 2, \dots, l \\ \|\tilde{\mathbf{w}}_i\|_{\mathbf{Q}} \text{ for } i = l + 1, l + 2 \dots, p \end{cases} & \quad (3.26) \\ \implies \min \|\mathbf{Y}^T - \boldsymbol{\Psi}(\mathbf{X})\tilde{\mathbf{W}}\|_F + \|\tilde{\mathbf{W}} - \tilde{\mathbf{W}}_0\|_{\mathbf{Q}} & \end{aligned}$$

where

$$\mathbf{W}^0 = \begin{bmatrix} | & & | & | & & | \\ \mathbf{w}_1^0 & \dots & \mathbf{w}_l^0 & 0 & \dots & 0 \\ | & & | & | & & | \end{bmatrix}, \quad \mathbf{Q} \succ 0,$$

is solved by

$$\tilde{\mathbf{W}} = (\mathbf{G} + \mathbf{Q})^{-1}(\mathbf{B} + \mathbf{Q}\mathbf{W}^0).$$

This can be used in our example problem. If the full state $\mathbf{y} = \mathbf{x}$ is considered alongside unknown outputs like in [37], we use $\mathbf{C} = \mathbf{I}_{n \times n}$ in our example dictionary and weight all dictionary functions equally using $\mathbf{Q} = \lambda \mathbf{I}_{n_L \times n_L}$. Then the expected output matrix is

$$\mathbf{W}^0 = \begin{bmatrix} \mathbf{I}_{n \times n} & 0 \\ 0 & 0 \end{bmatrix}$$

which gives the regularized minimizer $\tilde{\mathbf{W}} = (\mathbf{G} + \lambda \mathbf{I})^{-1}(\mathbf{B} + \lambda \mathbf{W}^0)$.

As stated earlier, even with linearly independent dictionary functions and sufficient data points for inversion, the above estimations of $\tilde{\mathbf{K}}, \tilde{\mathbf{W}}$ rely on the convergence of summations to inner products. Convergence with iid data was shown in [15] and the effect of sampling on independence of data was shown in [16]. Lastly, looking at dimensions, we see that $m \geq n_L \geq p$ with typical EDMD being $m > n_L \gg p$ [26].

Bibliography

- [1] I. Mezić and A. Banaszuk, “Comparison of systems with complex behavior,” *Physica D: Nonlinear Phenomena*, vol. 197, no. 1-2, pp. 101–133, 2004.
- [2] I. Mezić, “Spectral properties of dynamical systems, model reduction and decompositions,” *Nonlinear Dynamics*, vol. 41, no. 1-3, pp. 309–325, 2005.
- [3] B. O. Koopman, “Hamiltonian systems and transformation in hilbert space,” *Proceedings of the National Academy of Sciences of the United States of America*, vol. 17, no. 5, pp. 315–318, 1931.
- [4] P. J. Schmid, “Dynamic mode decomposition of numerical and experimental data,” *Journal of fluid mechanics*, vol. 656, pp. 5–28, 2010.
- [5] C. W. Rowley, I. Mezić, S. Bagheri, P. Schlatter, and D. S. Henningson, “Spectral analysis of nonlinear flows,” *Journal of fluid mechanics*, vol. 641, pp. 115–127, 2009.
- [6] M. O. Williams, I. G. Kevrekidis, and C. W. Rowley, “A data-driven approximation of the koopman operator: Extending dynamic mode decomposition,” *Journal of Nonlinear Science*, vol. 25, no. 6, pp. 1307–1346, 2015.
- [7] H. Arbabi and I. Mezić, “Ergodic theory, dynamic mode decomposition, and computation of spectral properties of the koopman operator,” *SIAM Journal on Applied Dynamical Systems*, vol. 16, no. 4, pp. 2096–2126, 2017.
- [8] I. Mezić, “Spectrum of the koopman operator, spectral expansions in functional spaces, and state-space geometry,” *Journal of Nonlinear Science*, pp. 1–55, 2019.
- [9] M. Korda and I. Mezić, “Optimal construction of koopman eigenfunctions for prediction and control,” *IEEE Transactions on Automatic Control*, 2020.
- [10] M. Korda and I. Mezić, “Linear predictors for nonlinear dynamical systems: Koopman operator meets model predictive control,” *Automatica*, vol. 93, pp. 149–160, 2018.
- [11] S. E. Otto and C. W. Rowley, “Koopman operators for estimation and control of dynamical systems,” *Annual Review of Control, Robotics, and Autonomous Systems*, vol. 4, pp. 59–87, 2021.

- [12] M. Korda, M. Putinar, and I. Mezić, “Data-driven spectral analysis of the koopman operator,” *Applied and Computational Harmonic Analysis*, 2018.
- [13] N. Črnjarić-Žic, S. Maćešić, and I. Mezić, “Koopman operator spectrum for random dynamical systems,” *Journal of Nonlinear Science*, pp. 1–50, 2019.
- [14] A. Mauroy, I. Mezić, and J. Moehlis, “Isostables, isochrons, and koopman spectrum for the action–angle representation of stable fixed point dynamics,” *Physica D: Nonlinear Phenomena*, vol. 261, pp. 19–30, 2013.
- [15] M. Korda and I. Mezić, “On convergence of extended dynamic mode decomposition to the koopman operator,” *Journal of Nonlinear Science*, vol. 28, no. 2, pp. 687–710, 2018.
- [16] N. Boddupalli, *Sparsification, sampling, and system identification in extended dynamic mode decomposition*. University of California, Santa Barbara, 2020.
- [17] N. Govindarajan, H. Arbabi, L. van Bargaian, T. Matchen, E. Tegling, *et al.*, “An operator-theoretic viewpoint to non-smooth dynamical systems: Koopman analysis of a hybrid pendulum,” in *2016 IEEE 55th Conference on Decision and Control (CDC)*, pp. 6477–6484, IEEE, 2016.
- [18] S. Peitz and S. Klus, “Koopman operator-based model reduction for switched-system control of pdes,” *Automatica*, vol. 106, pp. 184–191, 2019.
- [19] S. P. Banks, *State-space and frequency-domain methods in the control of distributed parameter systems*, vol. 3. Peter Peregrinus London, 1983.
- [20] A. Mauroy, Y. Susuki, and I. Mezić, “Introduction to the koopman operator in dynamical systems and control theory,” in *The Koopman Operator in Systems and Control*, pp. 3–33, Springer, 2020.
- [21] I. Mezić, “On numerical approximations of the koopman operator,” *arXiv preprint arXiv:2009.05883*, 2020.
- [22] M. Budišić, R. Mohr, and I. Mezić, “Applied koopmanism,” *Chaos: An Interdisciplinary Journal of Nonlinear Science*, vol. 22, no. 4, p. 047510, 2012.
- [23] D. G. Luenberger, *Optimization by vector space methods*. John Wiley & Sons, 1997.
- [24] J. L. Proctor, S. L. Brunton, and J. N. Kutz, “Generalizing koopman theory to allow for inputs and control,” *SIAM Journal on Applied Dynamical Systems*, vol. 17, no. 1, pp. 909–930, 2018.
- [25] P. Schmid and J. Sesterhenn, “Dynamic mode decomposition of numerical and experimental data,” *APS*, vol. 61, pp. MR–007, 2008.

- [26] M. O. Williams, C. W. Rowley, and I. G. Kevrekidis, “A kernel-based method for data-driven koopman spectral analysis,” *Journal of Computational Dynamics*, vol. 2, no. 2, p. 247, 2015.
- [27] J. A. Rosenfeld, R. Kamalapurkar, L. Gruss, and T. T. Johnson, “Dynamic mode decomposition for continuous time systems with the liouville operator,” *arXiv preprint arXiv:1910.03977*, 2019.
- [28] J. A. Rosenfeld and R. Kamalapurkar, “Dynamic mode decomposition with control liouville operators,” *arXiv preprint arXiv:2101.02620*, 2021.
- [29] A. E. Hoerl and R. W. Kennard, “Ridge regression: Biased estimation for nonorthogonal problems,” *Technometrics*, vol. 12, no. 1, pp. 55–67, 1970.
- [30] S. Boyd, S. P. Boyd, and L. Vandenberghe, *Convex optimization*. Cambridge university press, 2004.
- [31] C. A. Johnson and E. Yeung, “A class of logistic functions for approximating state-inclusive koopman operators,” in *2018 Annual American Control Conference (ACC)*, pp. 4803–4810, IEEE, 2018.
- [32] E. Yeung, S. Kundu, and N. Hodas, “Learning deep neural network representations for koopman operators of nonlinear dynamical systems,” in *2019 American Control Conference (ACC)*, pp. 4832–4839, IEEE, 2019.
- [33] B. Hanin, “Universal function approximation by deep neural nets with bounded width and relu activations,” *Mathematics*, vol. 7, no. 10, p. 992, 2019.
- [34] G. Cybenko, “Approximation by superpositions of a sigmoidal function,” *Mathematics of control, signals and systems*, vol. 2, no. 4, pp. 303–314, 1989.
- [35] J. Park and I. W. Sandberg, “Universal approximation using radial-basis-function networks,” *Neural computation*, vol. 3, no. 2, pp. 246–257, 1991.
- [36] G. H. Golub, P. C. Hansen, and D. P. O’Leary, “Tikhonov regularization and total least squares,” *SIAM journal on matrix analysis and applications*, vol. 21, no. 1, pp. 185–194, 1999.
- [37] S. Balakrishnan, A. Hasnain, R. Egbert, and E. Yeung, “The effect of sensor fusion on data-driven learning of koopman operators,” *arXiv preprint arXiv:2106.15091*, 2021.